Title: Endoplasmic reticulum stress and autophagy contribute to cadmium-induced cytotoxicity in retinal pigment epithelial cells

Authors: Lingmin Zhang, Qingqing Xia, Yingying Zhou, Jie Li

PII: S0378-4274(19)30134-1
DOI: https://doi.org/10.1016/j.toxlet.2019.05.001
Reference: TOXLET 10476

To appear in: *Toxicology Letters*

Received date: 5 July 2018
Revised date: 28 April 2019
Accepted date: 1 May 2019

Please cite this article as: Zhang L, Xia Q, Zhou Y, Li J, Endoplasmic reticulum stress and autophagy contribute to cadmium-induced cytotoxicity in retinal pigment epithelial cells, *Toxicology Letters* (2019), https://doi.org/10.1016/j.toxlet.2019.05.001

Endoplasmic reticulum stress and autophagy contribute to cadmium-induced cytotoxicity in retinal pigment epithelial cells

Lingmin Zhang [1], Qingqing Xia [1], Yingying Zhou, Jie Li *

Central Laboratory, Huangyan Hospital of Wenzhou Medical University, Taizhou First People's Hospital, Taizhou, Zhejiang Province, China.

[1]These authors contributed equally to this work.

*To whom correspondence should be addressed at: Central Laboratory, Huangyan Hospital of Wenzhou Medical University, Taizhou First People's Hospital, Taizhou, Zhejiang Province 318020, China.

E-mail: liyijie12580@126.com

Highlights:
•Cadmium-induced ROS causes apoptosis in RPE cells.
•ER stress contributes to cadmium-caused cytotoxicity.
•Cadmium-activated autophagy is detrimental in RPE cells.
•ER stress is involved in the regulation of Cadmium-induced autophagy in RPE cells.

Abstract:

Excessive accumulation of cadmium (Cd) in retina plays an important role in tobacco smoking-associated age-related macular degeneration (AMD). Plenty of evidence has revealed that the retinal pigment epithelium (RPE) is the primary site of pathology in AMD. Our current study demonstrated that Cd induced apoptosis in a human RPE cell line ARPE-19 cells, as it dose-dependently caused cell viability loss and activated caspase-3. The reactive oxygen species (ROS) were confirmed to be important mediators for Cd-triggered cell death in ARPE-19 cells. We found that endoplasmic reticulum (ER) stress was activated as its marker BiP was remarkably upregulated by Cd-exposure. Whereas the antioxidants N-acetylcysteine (NAC) and Tempol significantly suppressed the expression of BiP and CHOP, suggesting that ROS generation is an early trigger of Cd-activated ER stress. Furthermore, we found that Cd-induced oxidative stress significantly increased autophagic flux and p62 expression. A temporal impact of Cd exposure is possibly existed in p62 expression in ARPE-19 cells. Moreover, an ER stress inhibitor salubrinal diminished Cd-induced LC3BII expression and attenuated cytotoxicity, indicating that ER stress mediates autophagy and was implicated in apoptosis of Cd-exposed ARPE-19 cells. However, CHOP expression may not exert impact on the regulation of Cd-caused autophagy. Additionally, inhibition of autophagy with *si-Beclin 1* and 3-Methyladenine significantly ameliorated Cd-induced CHOP expression and cytotoxicity, indicating that autophagy was detrimental in Cd-accumulated ARPE-19 cells, and a positive feedback regulation mechanism may exist between Cd-triggered ER stress and autophagy. Taken together, these results suggest that Cd-caused ER stress and autophagy are implicated in RPE cell death associated retinopathies especially related to smoking.

Keywords:

Cadmium; retinal pigment epithelial cell; reactive oxygen species; ER-stress; autophagy

1. Introduction

Age-related macular degeneration (AMD) is a leading cause of blindness in elderly people worldwide (Lim et al., 2012). It is an ocular disease with complicated etiology and its exact pathogenesis remains obscure (Chu et al., 2013; Lim et al., 2012). In the retina, the retinal pigment epithelium (RPE) monolayer is essential for maintaining the normal visual transduction and especially vulnerable to damage. Thus it is thought to be the primary site of pathology in AMD (Ambati and Fowler, 2012; van Lookeren Campagne et al., 2014). Accumulated evidences strongly confirm cigarette smoking as a risk factor for this retinopathy (Lim et al., 2012; Woodell and Rohrer, 2014). Though the most important active ingredient of cigarette smoking in AMD has not been identified, a growing body of studies suggests that cadmium (Cd) may play a role in tobacco smoking-related AMD (Kalariya et al., 2009; Kim et al., 2014). Cd is concentrated in tobacco plants, thus cigarette smoking facilitate the Cd accumulation in the body. It was found that high blood Cd level is associated with AMD (Kim et al., 2014); and Cd level was approximately two folds of that in RPE of AMD eyes compared to non-AMD eyes (Wills et al., 2008).

Cd induces cytotoxicity in a variety of cell types, such as neurons, skin epidermal cells, renal proximal tubular cells, and RPE cells (Kalariya et al., 2009; Kim et al., 2013; Komoike et al., 2012; Son et al., 2011). A previous research demonstrated that Cd treatment triggered reactive oxygen species (ROS) generation and induced cell death in RPE cells (Kalariya et al., 2009); however, the underlying mechanisms have not been completely characterized. Studies have suggested that endoplasmic reticulum (ER) may be a major target organelle in Cd-exposed cells (Komoike et al., 2012; Luo et al., 2016). The ER homeostasis disruption results in ER stress, which has been implicated in the pathogenesis of several eye diseases such as retinitis pigmentosa, glaucoma, and

AMD (Li et al., 2015). Although ER stress has been proven to be associated with RPE dysfunction under certain circumstances, for example the intraretinal all-*trans*-retinal clearance interruption (Li et al., 2015), the role of ER stress in Cd-overladen RPE cells remains obscure and needs to be further clarified.

Plenty of works suggest that Cd exposure activates autophagy, which then promotes cell survival in certain cell type (Wang et al., 2013; Zou et al., 2015). On the contrary, Cd-induced autophagy also causes apoptosis in some kind of cells, such as skin epidermal cells and HEK cells (Luo et al., 2016; Son et al., 2011). Therefore, whether Cd-induced autophagy is salutary or detrimental is dependent on cell type. However, the role of Cd-induced autophagy in RPE cells remains unknown. Additionally, a resent research suggested that Cd-caused ER stress was involved in autophagy regulation (Luo et al., 2016). In contrast, in human renal proximal tubular cells, Cd-activated autophagy could not be affected by ER stress (Komoike et al., 2012). Thus, whether Cd-induced ER stress is implicated in autophagy-regulation may also depend upon cellular type.

The present study examined whether Cd exposure activates ER stress and autophagy in RPE cells, and delineated their roles in RPE cells. We found that upon Cd treatment, both ER stress and autophagy contribute to RPE cell death.

2. Materials and Methods

2.1. Reagents, antibodies and cell line

Cadmium chloride ($CdCl_2$), N-acetylcysteine (NAC), and chloroquine (CQ) were purchased from Aladdin (Shanghai, China) and prepared as stock solutions and stored at -20 °C. Salubrinal

(Sal) and thapsigargin (Tg) were obtained from Sigma-Aldrich (USA). 3-methyladenine (3-MA) and tempol were purchased from Selleck Chemicals (Shanghai, China). Primary antibodies rabbit anti-LC3B, rabbit anti-BiP, rabbit anti-cleaved caspase-3, mouse anti-GAPDH, and mouse anti-α-tubulin were purchased from cell signaling technology (USA). Rabbit anti-PARP1 and rabbit anti-CHOP were provided by proteintech company (USA). Rabbit anti-p62 was obtained from Abcam (UK). The human retinal pigment epithelial cell line ARPE-19 was obtained from FuDan IBS Cell Center (Shanghai, China). Cells were cultured in DMEM (Gibco, USA) with 10% fetal bovine serum (Gibco, USA) and 1% (v/v) penicillin/streptomycin in a humidified incubator (Thermo scientific, USA) at 37 °C and 5% CO_2.

2.2. Cell viability assay

Cytotoxicity of Cd was detected by MTT (Solabio, China) assay. Briefly, after incubation of ARPE-19 cells with various concentrations of $CdCl_2$ for 24 h, MTT solution was added to each culture well to achieve a final concentration of 0.5 mg/ml and incubated for 4 h. Then the medium was discarded and 150 μl DMSO was added to each well. The optical density (OD) value in each well was quantified at 490 nm with a microplate reader (Multiskan FC, Thermo scientific) after oscillating for 5 min. Cell viability was presented as a proportion of control optical density.

2.3. Analysis of ROS in RPE cells

The intracellular ROS level was estimated with dichloro-dihydro-fluorescein diacetate (DCFH-DA) (Beyotime, China) staining assay. After $CdCl_2$ treatment for 24 h, the medium was removed, and cells were incubated with 100 μl DMEM with 1 μM of ROS fluorescent probe in each well for 30 min at 37 °C. The medium was then discarded and cells were washed twice with

phosphate buffered saline (PBS) and subsequently observed and photographed with a fluorescence microscope (Olympus, Japan).

2.4. RNA extraction, cDNA synthesis and quantitative real-time PCR (qPCR)

Total RNA was extracted and purified using TRIzol reagent (Invitrogen Inc., Carlsbad, CA). The RNA purity and concentration were determined by a Tgem spectrophotometer (Tiangen, China). cDNA was synthesized with a ReverTra Ace® qPCR RT kit (TOYOBO). qPCR was carried out on an ABI Prism® 7500 real-time PCR detection system (Applied Biosystems, USA) using Brilliant SYBR Green qPCR Master Mix reagent with ROX reference dye (TakaRa). Each qPCR was performed on three different experimental samples and each sample was performed in triplicate. Reactions without cDNA template served as negative controls. The relative expression level of each target gene was calculated with the $2^{-\Delta\Delta Ct}$ method (Livak and Schmittgen, 2001) using *GAPDH* as a loading control. The following primer sequences were used: *HO-1*, 5'-CCAGCGGGCCAGCAACAAAGTGC-3', 5'- AAGCCTTCAGTGCCCACGGTAAGG-3' (Colombrita et al., 2003); *BiP*, 5'-GCCTGTATTTCTAGACCTGCC-3', 5'-TTCATCTTGCCAGCCAGTTG-3' (Nakamura et al., 2013); *CHOP*, 5'-GACCTGCAAGAGGTCCTGTC-3', 5'-TGTGACCTCTGCTGGTTCTG-3' (Nakamura et al., 2013); *GAPDH*, 5'-TGACGCTGGGGCTGGCATTG-3', 5'-GGCTGGTGGTCCAGGGGTCT-3' (Li et al., 2015).

2.5. Autophagic flux measurement

ARPE-19 cells were infected with recombinant adeno-associated virus vectors packing mCherry-eGFP-LC3B (Vigene Biosciences, Shandong, China) according to the manufacturer's instructions. Briefly, ARPE-19 cells were seeded at close to 50% confluence without any

antibiotics in a 24-well cell culture plate. 24 h later, 1 μl of recombinant adeno-associated virus (3.2×10^{10} pfu/ml) was added into each well. After 24 h post-infection, cells were exposed to Cd for 24 h and analyzed by fluorescence microscopy.

2.6. Morphological analysis after DAPI staining

After fixed with 4% paraformaldehyde for 15 min at room temperature, ARPE-19 cell nuclei were stained with DAPI for 5 min in the dark. Then cells were washed with PBS for three times and analyzed by fluorescence microscopy (CKX53, Olympus, Japan). The normal cell nucleus is round, clear-edged, and uniformly stained, whereas the apoptotic cells show irregular edges around the nucleus, heavier staining, and nuclear pyknosis. Three to seven views from each well were photographed for apoptotic cells counting, and the ratio of condensed nuclei/total nuclei was calculated and expressed as apoptosis rate in each group.

2.7. siRNA transfection.

CHOP siRNA (5'-GGUCCUGUCUUCAGAUGAATT-3'), *Beclin-1* siRNA (5'-GGUCUAAGACGUCCAACAATT-3') and a negative control (NC) (5'-GCGACGAUCUGCCUAAGAUdTdT-3') were designed and synthesized by GenePharma Company (Shanghai, China). ARPE-19 cells were seeded at close to 30% confluence without any antibiotics. 24 h later, specific siRNA or NC (100 nM) was added into cells with Lipofectamine 3000 according to the manufacturer's instructions.

2.8. Western blot analysis

Cellular proteins were prepared with RIPA lysis buffer (Beyotime) that contains 1% protease inhibitor cocktails (Hangzhou fude biological technology, China) and the protein concentration was quantified using an enhanced BCA protein assay kit (Beyotime). After denaturation, proteins

were separated by SDS-PAGE denaturing gel electrophoresis and then transferred to PVDF membrane (Millipore, USA). The membrane was blocked with 5% skim milk for 1 h at room temperature and rinsed in wash buffer. Each membrane was subsequently incubated with the specific primary antibody overnight at 4 °C. Membranes were washed three times and incubated with the corresponding horseradish peroxidase-conjugated secondary antibody (Beyotime) for 1 h at room temperature. The results were visualized with a BeyoECL kit (Beyotime) and analyzed on the ChemiDox^{TM} XRS+ system (Bio-rad, USA) with Image Lab^{TM} software.

2.9. Statistical analysis

All data were expressed as the means ± SEM and analyzed by one-way analysis of variance, followed by Newman-Keuls test for multiple comparisons. $P < 0.05$ was accepted as a statistically significant difference.

3. Results

3.1. Cd induced apoptosis via oxidative stress in RPE cells.

Cell viability in ARPE-19 cells were examined after incubation with $CdCl_2$ (0-40 μM) for 24 h. As shown in Fig. 1A, 5 μM $CdCl_2$ appeared to produce no cytotoxicity in ARPE-19 cells; however, 10, 20, and 40 μM $CdCl_2$ significantly decreased cell viability by approximately 15%, 25% and 32%, respectively. We also found a significant up-regulation of cleaved fragment of caspase-3 (Fig. 1B), which is a critical executioner of apoptosis. This demonstrates that $CdCl_2$ may activate apoptosis in RPE cells through the caspase-dependent apoptotic pathway. The intracellular ROS level was evaluated after $CdCl_2$ treatment by DCFH-DA staining. Compared to the control cells, $CdCl_2$ provoked ROS generation in a dose-dependent manner after 24 h incubation (Fig. 1C).

Heme oxygenase-1 (HO-1) is highly inducible by oxidative stress, and is considered as an important intracellular antioxidant (Li et al., 2015). qPCR analysis found that mRNA expression levels of *HO-1* was significantly increased after $CdCl_2$ (0-20 μM) incubation (Fig. 1D).

Tempol and NAC were widely used as free radicals quenchers (Li et al., 2015; Liu et al., 2014). To clarify whether Tempol and NAC could attenuate Cd-induced cell cytotoxicity, the expression of cleaved PARP1, which is one of the caspase-3 downstream effectors, was detected by immunoblotting. As depicted in Figure 1E and F, Cd-caused cleaved PARP1 expression was markedly suppressed by NAC pre-incubation or Tempol addition. We also observed the cell morphology changes after NAC pretreatment. As shown in Fig. 1G, after exposure to 20 μM $CdCl_2$ for 24 h, RPE cells were severely damaged, and many cells were round and shrunken, and in the process of dying, but 2 mM NAC significantly inhibited Cd-caused RPE cell damage. These results confirm that ROS is the crucial mediator for Cd-triggered in RPE cell death.

3.2. Cd activated ER stress in RPE cells.

The ER-resident molecular chaperone BiP, which is widely used as a marker of ER stress, was increased in both dose- and time-dependent manners after Cd incubation (Fig. 2A and B). We then detected the mRNA expression levels of *BiP*, *ATF4*, and *CHOP* by qPCR, and found that *BiP* and *CHOP* were up-regulated with the increasing of Cd concentrations (Fig. 2C, E). Western blot analysis also showed that CHOP expression was raised in a dose-dependent manner with Cd treatment for 24 h (Fig. 2F). The expression level of *ATF4* was not affected by 20 μM $CdCl_2$ exposure; however, in comparison with that in the control, there was approximately a 30% increase with either 5 or 10 μM $CdCl_2$ incubation, and they were statistically significant (Fig. 2D). Moreover, we found that NAC or Tempol treatment dramatically suppressed Cd-caused

up-regulation of BiP and CHOP (Fig. 2G and H). These results imply that Cd-induced oxidative stress caused ER stress in RPE cells.

3.3. Cd activated autophagy flux in RPE cells.

LC3 is the structural protein of autophagosomal membranes and expressed as four isoforms (LC3A, LC3B, LC3B2 and LC3C) in mammalian cells (Srinivasula et al., 2015). LC3II is derived from LC3I during autophagy and is widely used as a marker for autophagosomes. As shown in Fig. 3A and C, LC3BII was remarkably up-regulated as a function of both exposure time and $CdCl_2$ concentration. In addition to LC3, the multi-functional scaffold protein p62, which also serves as a link between LC3 and ubiquitinated substrates, is used as an index of autophagy degradation (Mizunoe et al., 2018; Song et al., 2017). Interestingly, our results demonstrated that after Cd exposure in RPE cells for 24 h, p62 protein expression was obviously increased (Fig. 3B). Meanwhile, short time (1 h) incubation of 20 μM $CdCl_2$ significantly decreased p62 level (Fig. 3C). However, the protein level was gradually increased and was maximal after incubation for 12 h or 24 h (Fig. 3C) in comparison with that in the control. To further examine the effects of Cd on autophagic p62 degradation, we conducted the LC3BII turnover assay which has recently been widely used to analyze autophagic flux (Mizushima et al., 2010). In this assay, we found that pretreatment of CQ, an inhibitor of lysosomal acidification and autophagic clearance, augmented both LC3BII and p62 accumulation in 24 h Cd-treated cells (Fig. 3D and E). Furthermore, we infected ARPE-19 cells with recombinant adeno-associated virus vectors packing tandem sensor mCherry-eGFP-LC3B construct to investigate autophagic flux in more detail (Mizunoe et al., 2018; Thoen et al., 2011). The green fluorescent signal of eGFP is easily quenched under low pH circumstances inside the lysosomes. In contrast, mCherry exhibits more stable fluorescence in

acidic compartments. Thus, the mCherry-eGFP-LC3B fusion protein enabled discrimination between autophagosomes exhibiting yellow fluorescence and autolysosomes exhibiting only red signal (Mizunoe et al., 2018; Thoen et al., 2011). Our data manifested that 24 h Cd incubation markedly increased the number of cells with more red puncta (white arrow heads), while CQ pretreatment yielded more cells exhibiting yellow signal and significantly decreased the number of red-fluorescent RPE cells after Cd exposure (Fig. 3G), indicating that Cd functionally activated autophagy. Moreover, we found that Tempol incubation obviously attenuated Cd-induced LC3BII expression (Fig. 3F), suggesting that Cd-activated autophagy is ROS-dependent.

3.4. ER stress contributed to Cd-induced autophagy and cytotoxicity in RPE cells.

We then investigated whether inhibition of ER stress with salubrinal (Sal), which is a widely used ER stress inhibitor (Boyce, 2005), could affect Cd-caused autophagy and cytotoxicity. Our data demonstrated that salubrinal (20 and 40 μM) pretreatment dose-dependently reduced Cd-induced LC3BII expression (Fig. 4A), and inhibited the expression of Beclin 1 (Fig. 4C), which plays a crucial role in autophagosome formation (Wei et al., 2013). Salubrinal suppressed CHOP up-regulation (Fig. 4C), but provoked BiP expression in Cd-exposed RPE cells (Fig. 4B). Condensed nuclei of ARPE-19 cells after exposure to $CdCl_2$ for 24 h were determined by DAPI staining, the number of pyknotic nuclei was significantly increased with $CdCl_2$ incubation (Fig. 4D, white arrowheads). The present results demonstrated that salubrinal markedly attenuated Cd-induced apoptosis (Fig. 4E). Besides, we also investigated the role of CHOP in autophagy induction, we observed that siRNA knockdown of CHOP could not affect LC3BII expression (Fig. 4F), but suppressed the activation of PARP1 (Fig. 4G). Furthermore, Thapsigargin (Tg, an inhibitor of ER Ca^{2+} uptake), which is widely used as an ER stress inducer (Zhang et al., 2014),

was employed to investigate the relationship between ER stress and autophagy or apoptosis. Our results demonstrated that inclusion of 1 μM Tg in RPE cells treated with 20 μM $CdCl_2$ up-regulated the expression levels of CHOP, LC3BII, and cleaved PARP1 (Fig. 4H). Taken together, these results suggest that ER stress is implicated in Cd-activated autophagy and cytotoxicity in RPE cells.

3.5. Autophagy was involved in Cd-caused RPE cell death.

To determine whether autophagy promotes cell survival or cell death, we inhibited autophagy by *si-Beclin 1* or 3-MA. We found that siRNA knockdown of Beclin 1 prevented Cd-caused increases of LC3BII and CHOP (Fig. 5A). Condensed nuclei of ARPE-19 cells were determined by DAPI staining, and the number of pyknotic nuclei was dramatically increased with $CdCl_2$ incubation (Fig. 5B, white arrowheads), whereas *si-Beclin 1* significantly attenuated Cd-induced apoptosis (Fig. 5C). Similarly, the autophagic sequestration inhibitor 3-MA also reduced Cd-induced CHOP expression and caspase 3 activation; and prevented Cd-caused cytotoxicity (Fig. 5D and E). Trehalose (Tre) is a novel autophagy enhancer (Wang et al., 2017). To further clarify the role of autophagy in Cd-exposed RPE cells, we treated RPE cells with $CdCl_2$ in the presence or absence of 50 mM Trehalose for 24 h. As shown in Fig. 5F, Trehalose incubation markedly increased expressions of Cd-activated LC3BII, CHOP, and cleaved PARP1.

4. Discussion

Tobacco smoking is the only proven, strong and consistent risk factor for AMD (Lim et al., 2012; Woodell and Rohrer, 2014). It contains more than 4800 compounds, of which heavy metal Cd was suggested to be a possible contributor to smoking-related AMD (Chu et al., 2013; Kalariya

et al., 2009; Kim et al., 2014; Wills et al., 2008). Our work confirmed that Cd exposure induced cell viability inhibition, and caused cell apoptosis (Fig. 1A and B). Also our results suggested that oxidative insults were implicated in Cd-caused RPE cell death (Fig. 1C-G). These findings are consistent with a previously reported research and confirm that ROS-quenching attenuates Cd-triggered cytotoxicity in RPE cells (Kalariya et al., 2009).

Besides apoptosis, a diverse range of cellular activities including intercellular communication, energy homoeostasis, and necrosis have reported to be affected upon Cd exposure (Chen et al., 2015; Kim et al., 2013; Messner et al., 2016; Zou et al., 2015). Our present results showed that Cd incubation functionally activated autophagic flux, accompanied by an increased p62 expression in RPE cells (Fig. 3). Moreover, a temporal impact of Cd exposure is possibly existed in p62 expression (Fig. 3C), and our findings suggested that the deposition of p62 in RPE cells after 24 h Cd incubation was not due to lysosomal clearance defect (Fig. 3B, C, E, and G). It has recently been demonstrated that oxidative stress causes elevated p62 expression in RPE cells, and p62 is closely involved in the regulation of the Nrf2/ARE antioxidant defense pathway (Koskela et al., 2016; Song et al., 2017). Given that Cd exposure can strongly activate the Nrf2/ARE pathway (Shinkai et al., 2016), together with the findings in Fig. 1, we think that Cd-induced oxidative stress might be the reason for Cd-caused p62 accumulation in RPE cells.

Subsequently, we found that oxidative stress may also be responsible for the activation of autophagy (Fig. 3F). Plenty of literatures have demonstrated that autophagy may relieve cell oxidative stress by initiating a self-degradative process for the removal of misfolded proteins and damaged organelles (Salcher et al., 2017). However, it may also contribute to cell apoptosis through excessive self-digestion and degradation of essential cellular constituents (So et al., 2018;

Son et al., 2011). Our results demonstrated that suppression of autophagy with pharmacological and RNA interference approaches significantly attenuated Cd-caused cytotoxicity (Fig. 5B, C, and E). By contrast, Trehalose promoted Cd-caused autophagy and aggravated cell apoptosis (Fig. 5F), confirming that autophagy is detrimental in Cd-accumulated RPE cells.

Released from the ER resident proteins PERK, IRE1, or ATF6, the molecular chaperone BiP prevents protein aggregation and helps them fold properly. BiP is not only a pro-survival factor, but also widely used as a marker of ER stress (Lebeau et al., 2018; Li et al., 2015). The expression elevation of BiP suggested that ER stress was activated in Cd-treated RPE cells (Fig 2A-C). The transcriptional level of *ATF4*, however, is not very sensitive to Cd-induced stress in RPE cells (Fig. 2D). Nevertheless, we found that CHOP, which is a downstream transcription factor of ATF4 and closely associated with ROS generation and ER stress-related cell apoptosis (Lee et al., 2018; Li et al., 2015), was remarkably elevated in Cd-treated RPE cells (Fig. 2E and F). Previously published studies have revealed that ER may be a target organelle of ROS (Li et al., 2015; Naranmandura et al., 2012). Consistently, our current findings demonstrated that partial quenching of intracellular ROS with antioxidant NAC or Tempol significantly suppressed Cd-induced BiP and CHOP up-regulation (Fig. 2G and H), indicating that Cd-caused ER stress is mediated by intracellular ROS overproduction.

Although emerging evidence reveals that ER stress may act as an adaptive response to maintain cellular homeostasis and promote cell survival, extensive ER dysfunction is also detrimental (Li et al., 2017). Salubrinal is an established ER stress inhibitor which can rescue cells from tunicamycin-induced apoptosis by inhibiting eIF2a dephosphorylation (Boyce, 2005). Therefore, we used salubrinal to suppress ER stress and clarify its role in Cd-caused apoptosis.

Our data showed that salubrinal increased the expression level of the pro-survival protein BiP (Song et al., 2018b), but significantly inhibited CHOP up-regulation (Fig. 4B and C). As a result, salubrinal significantly alleviates the cytotoxicity of Cd exposure in RPE cells (Fig. 4D and E). ER stress-related molecular events, like up-regulated CHOP, provokes intracellular ROS production, and induced apoptosis by BCL2 inhibition and Bim induction (Li et al., 2015). Consistently, we found that siRNA knockdown of CHOP attenuated the cleavage of PARP1 (Fig.4G), indicating that CHOP may play a role in Cd-induced RPE cell apoptosis. Previous researches have also revealed that ER stress-activated caspase 4 or caspase 12 initiated cell apoptosis (Li et al., 2015; Song et al., 2018a). Furthermore, we found that ER stress inducer Tg aggravated Cd-caused CHOP expression, and increased PARP1 activation (Fig. 4H), confirming that ER stress contributes to Cd-caused cytotoxicity in RPE cells. Our data, together with a lot of published results (Komoike et al., 2012; Luo et al., 2016), strengthen the idea that the ER may be a major target organelle of Cd exposure.

Salubrinal pretreatment abolished ER stress and alleviated Cd-caused LC3BII increase (Fig. 4A and C), whereas aggravation of ER stress with Tg accelerated its expression (Fig. 4H). Mounting evidence suggest that ER is closely associated with autophagy induction, since the activation of autophagy can facilitate the degradation of accumulated misfolded or unfolded proteins result from ER stress (Ogata et al., 2006; Zhang et al., 2014), and ER is the potential membrane source of autophagosome and provides calcium signaling for autophagy initiation (Holowka et al., 2013; Tooze and Yoshimori, 2010). Consistent with these findings, our results indicated that Cd-induced ER stress may be implicated in autophagy induction (Fig. 4A, C, and H).

However, as shown in Fig. 4F, CHOP inhibition could not affect the expression of LC3BII, indicating that CHOP expression may not exert impact on the regulation of Cd-caused autophagy.

Suppression of autophagy inhibited Cd-caused cytotoxicity, and simultaneously abolished CHOP expression (Fig. 5A-E). Additionally, exacerbation of autophagy with Trehalose aggravated Cd-induced CHOP upregulation and ER stress (Fig. 5F), indicating that a positive feedback regulation mechanism may exist between Cd-triggered ER stress and autophagy. Cd-caused excessive activation of autophagy may worsen cellular homeostasis disruption, thus promoting ER dysfunction and enhancing ER stress.

In summary, our study demonstrated that Cd-induced ROS activated ER stress, autophagy, and apoptosis in RPE cells. Both ER stress and autophagy are involved in Cd-associated RPE cell death. Moreover, Cd-induced ER stress mediates autophagy, and a positive feedback regulation mechanism may exist between autophagy and ER stress. These results indicate that ER stress or autophagy inhibitor or their combination may be effective in protection RPE cells against Cd-induced cytotoxicity. This study expands our understanding in Cd-caused RPE cell death associated retinopathies especially related to smoking.

Acknowledgments

The present study was supported by the Medical Science and Technology Program of Zhejiang Province (2016KYA195 and 2017KY714); Zhejiang Provincial Natural Science Foundation of China (LQ17H120001); the National Natural Science Foundation of China (81801424); and the 211 talents training program of Taizhou (Jie Li).

References

Ambati, J., Fowler, Benjamin J., 2012. Mechanisms of Age-Related Macular Degeneration. Neuron 75, 26-39.

Boyce, M., 2005. A Selective Inhibitor of eIF2 Dephosphorylation Protects Cells from ER Stress. Science 307, 935-939.

Chen, C.Y., Zhang, S.L., Liu, Z.Y., Tian, Y., Sun, Q., 2015. Cadmium toxicity induces ER stress and apoptosis via impairing energy homoeostasis in cardiomyocytes. Bioscience reports 35.

Chu, Y.K., Lee, S.C., Byeon, S.H., 2013. VEGF rescues cigarette smoking-induced human RPE cell death by increasing autophagic flux: implications of the role of autophagy in advanced age-related macular degeneration. Investigative ophthalmology & visual science 54, 7329-7337.

Colombrita, C., Lombardo, G., Scapagnini, G., Abraham, N.G., 2003. Heme oxygenase-1 expression levels are cell cycle dependent. Biochemical and biophysical research communications 308, 1001-1008.

Holowka, D., Decuypere, J.-P., Kindt, D., Luyten, T., Welkenhuyzen, K., Missiaen, L., De Smedt, H., Bultynck, G., Parys, J.B., 2013. mTOR-Controlled Autophagy Requires Intracellular Ca2+ Signaling. PLoS ONE 8, e61020.

Kalariya, N.M., Wills, N.K., Ramana, K.V., Srivastava, S.K., van Kuijk, F.J., 2009. Cadmium-induced apoptotic death of human retinal pigment epithelial cells is mediated by MAPK pathway. Experimental eye research 89, 494-502.

Kim, E.C., Cho, E., Jee, D., 2014. Association Between Blood Cadmium Level and Age-Related Macular Degeneration in a Representative Korean Population. Investigative Opthalmology & Visual Science 55, 5702.

Kim, S., Cheon, H.S., Kim, S.Y., Juhnn, Y.S., Kim, Y.Y., 2013. Cadmium induces neuronal cell death through reactive oxygen species activated by GADD153. Bmc Cell Biol 14.

Komoike, Y., Inamura, H., Matsuoka, M., 2012. Effects of salubrinal on cadmium-induced apoptosis in HK-2 human renal proximal tubular cells. Arch Toxicol 86, 37-44.

Koskela, A., Reinisalo, M., Petrovski, G., Sinha, D., Olmiere, C., Karjalainen, R., Kaarniranta, K., 2016. Nutraceutical with Resveratrol and Omega-3 Fatty Acids Induces Autophagy in ARPE-19 Cells. Nutrients 8.

Lebeau, P., Platko, K., Al-Hashimi, A.A., Byun, J.H., Lhoták, Š., Holzapfel, N., Gyulay, G., Igdoura, S.A., Cool, D., Trigatti, B., Seidah, N.G., Austin, R.C., 2018. Loss-of-function PCSK9 mutants evade the unfolded protein response sensor, GRP78, and fail to induce endoplasmic reticulum stress when retained. Journal of Biological Chemistry, jbc.RA117.001049.

Lee, Y.-S., Lee, D.-H., Choudry, H.A., Bartlett, D.L., Lee, Y.J., 2018. Ferroptosis-induced Endoplasmic Reticulum Stress: Crosstalk Between Ferroptosis and Apoptosis. Molecular Cancer Research, molcanres.0055.2018.

Li, J., Cai, X., Xia, Q., Yao, K., Chen, J., Zhang, Y., Naranmandura, H., Liu, X., Wu, Y., 2015. Involvement of Endoplasmic Reticulum Stress in All-Trans-Retinal-Induced Retinal Pigment

Epithelium Degeneration. Toxicological Sciences 143, 196-208.

Li, J., Zhang, L., Xia, Q., Fu, J., Zhou, Z., Lin, F., 2017. Hedgehog signaling inhibitor GANT61 induces endoplasmic reticulum stress-mediated protective autophagy in hepatic stellate cells. Biochemical and biophysical research communications 493, 487-493.

Lim, L.S., Mitchell, P., Seddon, J.M., Holz, F.G., Wong, T.Y., 2012. Age-related macular degeneration. The Lancet 379, 1728-1738.

Liu, Y., Shim, E., Nguyen, P., Gibbons, A.T., Mitchell, J.B., Poirier, M.C., 2014. Tempol Protects Cardiomyocytes from Nucleoside Reverse Transcriptase Inhibitor-Induced Mitochondrial Toxicity. Toxicological Sciences 139, 133-141.

Livak, K.J., Schmittgen, T.D., 2001. Analysis of relative gene expression data using real-time quantitative PCR and the $2^{-\Delta\Delta CT}$ method. Methods 25, 402-408.

Luo, B., Lin, Y., Jiang, S., Huang, L., Yao, H., Zhuang, Q., Zhao, R., Liu, H., He, C., Lin, Z., 2016. Endoplasmic reticulum stress eIF2alpha-ATF4 pathway-mediated cyclooxygenase-2 induction regulates cadmium-induced autophagy in kidney. Cell death & disease 7, e2251.

Messner, B., Turkcan, A., Ploner, C., Laufer, G., Bernhard, D., 2016. Cadmium overkill: autophagy, apoptosis and necrosis signalling in endothelial cells exposed to cadmium. Cellular and molecular life sciences : CMLS 73, 1699-1713.

Mizunoe, Y., Kobayashi, M., Sudo, Y., Watanabe, S., Yasukawa, H., Natori, D., Hoshino, A., Negishi, A., Okita, N., Komatsu, M., Higami, Y., 2018. Trehalose protects against oxidative stress by regulating the Keap1-Nrf2 and autophagy pathways. Redox biology 15, 115-124.

Mizushima, N., Yoshimori, T., Levine, B., 2010. Methods in mammalian autophagy research. Cell 140, 313-326.

Nakamura, S., Takizawa, H., Shimazawa, M., Hashimoto, Y., Sugitani, S., Tsuruma, K., Hara, H., 2013. Mild Endoplasmic Reticulum Stress Promotes Retinal Neovascularization via Induction of BiP/GRP78. PLoS ONE 8, e60517.

Naranmandura, H., Xu, S., Koike, S., Pan, L.Q., Chen, B., Wang, Y.W., Rehman, K., Wu, B., Chen, Z., Suzuki, N., 2012. The endoplasmic reticulum is a target organelle for trivalent dimethylarsinic acid (DMAIII)-induced cytotoxicity. Toxicology and applied pharmacology 260, 241-249.

Ogata, M., Hino, S.i., Saito, A., Morikawa, K., Kondo, S., Kanemoto, S., Murakami, T., Taniguchi, M., Tanii, I., Yoshinaga, K., Shiosaka, S., Hammarback, J.A., Urano, F., Imaizumi, K., 2006. Autophagy Is Activated for Cell Survival after Endoplasmic Reticulum Stress. Molecular and Cellular Biology 26, 9220-9231.

Salcher, S., Hermann, M., Kiechl-Kohlendorfer, U., Ausserlechner, M.J., Obexer, P., 2017. C10ORF10/DEPP-mediated ROS accumulation is a critical modulator of FOXO3-induced autophagy. Molecular Cancer 16.

Shinkai, Y., Kimura, T., Itagaki, A., Yamamoto, C., Taguchi, K., Yamamoto, M., Kumagai, Y., Kaji, T., 2016. Partial contribution of the Keap1-Nrf2 system to cadmium-mediated metallothionein expression in vascular endothelial cells. Toxicology and applied pharmacology 295, 37-46.

So, K.-Y., Lee, B.-H., Oh, S.-H., 2018. The critical role of autophagy in cadmium-induced immunosuppression regulated by endoplasmic reticulum stress-mediated calpain activation in RAW264.7 mouse monocytes. Toxicology 393, 15-25.

Son, Y.O., Wang, X., Hitron, J.A., Zhang, Z., Cheng, S., Budhraja, A., Ding, S., Lee, J.C., Shi, X.,

2011. Cadmium induces autophagy through ROS-dependent activation of the LKB1-AMPK signaling in skin epidermal cells. Toxicology and applied pharmacology 255, 287-296.

Song, C., Mitter, S.K., Qi, X., Beli, E., Rao, H.V., Ding, J., Ip, C.S., Gu, H., Akin, D., Dunn, W.A., Jr., Bowes Rickman, C., Lewin, A.S., Grant, M.B., Boulton, M.E., 2017. Oxidative stress-mediated NFkappaB phosphorylation upregulates p62/SQSTM1 and promotes retinal pigmented epithelial cell survival through increased autophagy. PLoS One 12, e0171940.

Song, J., Zhang, Q., Wang, S., Yang, F., Chen, Z., Dong, Q., Ji, Q., Yuan, X., Ren, D., 2018a. Cleavage of caspase-12 at Asp94, mediated by endoplasmic reticulum stress (ERS), contributes to stretch-induced apoptosis of myoblasts. Journal of Cellular Physiology 233, 9473-9487.

Song, X., Lee, D.H., Dilly, A.K., Lee, Y.S., Choudry, H.A., Kwon, Y.T., Bartlett, D.L., Lee, Y.J., 2018b. Crosstalk Between Apoptosis and Autophagy Is Regulated by the Arginylated BiP/Beclin-1/p62 Complex. Molecular cancer research : MCR 16, 1077-1091.

Srinivasula, S.M., Koukourakis, M.I., Kalamida, D., Giatromanolaki, A., Zois, C.E., Sivridis, E., Pouliliou, S., Mitrakas, A., Gatter, K.C., Harris, A.L., 2015. Autophagosome Proteins LC3A, LC3B and LC3C Have Distinct Subcellular Distribution Kinetics and Expression in Cancer Cell Lines. Plos One 10, e0137675.

Thoen, L.F., Guimaraes, E.L., Dolle, L., Mannaerts, I., Najimi, M., Sokal, E., van Grunsven, L.A., 2011. A role for autophagy during hepatic stellate cell activation. Journal of hepatology 55, 1353-1360.

Tooze, S.A., Yoshimori, T., 2010. The origin of the autophagosomal membrane. Nature Cell Biology 12, 831-835.

van Lookeren Campagne, M., LeCouter, J., Yaspan, B.L., Ye, W., 2014. Mechanisms of age-related macular degeneration and therapeutic opportunities. The Journal of Pathology 232, 151-164.

Wang, Q., Zhu, J., Zhang, K., Jiang, C., Wang, Y., Yuan, Y., Bian, J., Liu, X., Gu, J., Liu, Z., 2013. Induction of cytoprotective autophagy in PC-12 cells by cadmium. Biochemical and biophysical research communications 438, 186-192.

Wang, X.-Y., Yang, H., Wang, M.-G., Yang, D.-B., Wang, Z.-Y., Wang, L., 2017. Trehalose protects against cadmium-induced cytotoxicity in primary rat proximal tubular cells via inhibiting apoptosis and restoring autophagic flux. Cell Death and Disease 8, e3099.

Wei, Y., Zou, Z., Becker, N., Anderson, M., Sumpter, R., Xiao, G., Kinch, L., Koduru, P., Christudass, Christhunesa S., Veltri, Robert W., Grishin, Nick V., Peyton, M., Minna, J., Bhagat, G., Levine, B., 2013. EGFR-Mediated Beclin 1 Phosphorylation in Autophagy Suppression, Tumor Progression, and Tumor Chemoresistance. Cell 154, 1269-1284.

Wills, N.K., Ramanujam, V.M.S., Chang, J., Kalariya, N., Lewis, J.R., Weng, T.X., van Kuijk, F.J.G.M., 2008. Cadmium accumulation in the human retina: Effects of age, gender, and cellular toxicity. Experimental eye research 86, 41-51.

Woodell, A., Rohrer, B., 2014. A mechanistic review of cigarette smoke and age-related macular degeneration. Advances in experimental medicine and biology 801, 301-307.

Zhang, X., Yuan, Y., Jiang, L., Zhang, J., Gao, J., Shen, Z., Zheng, Y., Deng, T., Yan, H., Li, W., Hou, W.-W., Lu, J., Shen, Y., Dai, H., Hu, W.-W., Zhang, Z., Chen, Z., 2014. Endoplasmic reticulum stress induced by tunicamycin and thapsigargin protects against transient ischemic brain injury. Autophagy 10, 1801-1813.

Zou, H., Zhuo, L., Han, T., Hu, D., Yang, X., Wang, Y., Yuan, Y., Gu, J., Bian, J., Liu, X., Liu, Z., 2015. Autophagy and gap junctional intercellular communication inhibition are involved in cadmium-induced apoptosis in rat liver cells. Biochemical and biophysical research communications 459, 713-719.

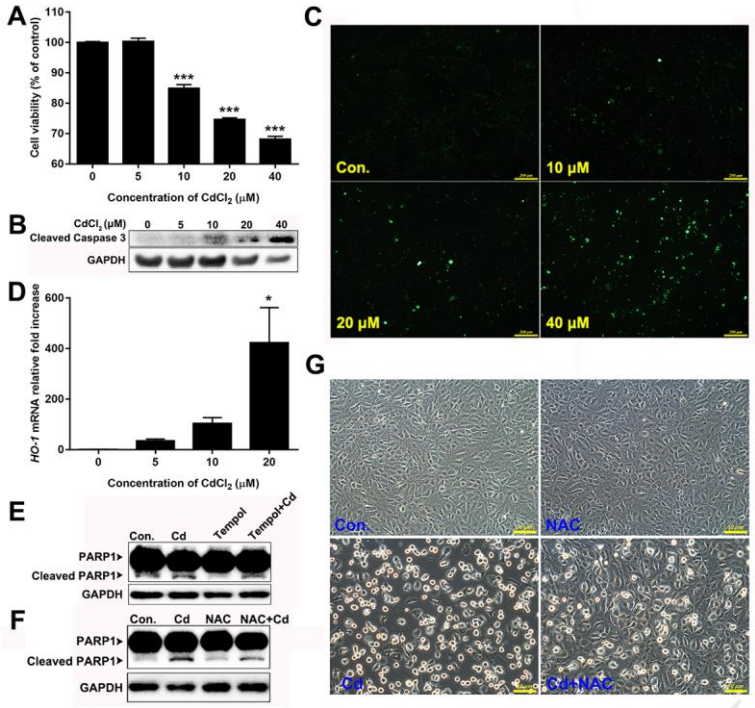

Fig. 1. Cd causes ROS generation, cell viability loss and apoptosis in RPE cells.

(A) ARPE-19 cells were exposed to various concentrations (0-40 μM) of $CdCl_2$ for 24 h and cell viability was evaluated by MTT assay. Each value represents means ± SEM (n=6). ***$P < 0.001$. (B) After ARPE-19 cells were incubated with $CdCl_2$ (0-40 μM) for 24 h, total cell lysates were analyzed by western blotting using indicated antibodies. (C) Intracellular ROS was visualized by fluorescence microscopy. Scale bar, 200 μm. (D) mRNA expression was quantified for *HO-1* using qPCR. Each value is presented as mean ± SEM of 3 independent experiments. *$P < 0.05$. (E) PARP1 was detected by western blotting after ARPE-19 cells were subjected to 20 μM $CdCl_2$ for 24 h in the absence or presence of 2 mM Tempol. (F and G) ARPE-19 cells were pretreated with NAC (2 mM) for 2 h and washed with PBS for three times, then were exposed to 20 μM $CdCl_2$ for 24 h. Subsequently, total cell lysates were detected by western blotting using indicated

antibodies (F), and the morphologic changes were observed and photographed under an inverted microscope (G). Scale bar, 50 μm; Con., Control.

(B)

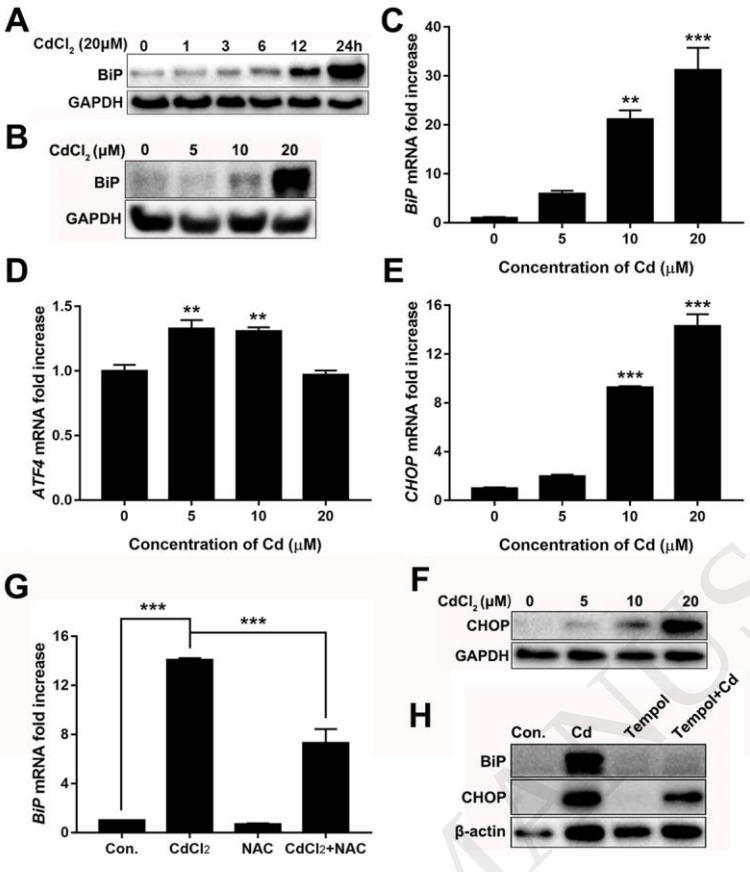

(C)

Fig. 2. Cd activates ER stress in ARPE-19 cells

BiP expression was determined by western blotting after ARPE-19 cells were treated with $CdCl_2$ (0, 5, 10, and 20 μM) for 24 h (A) or 20 μM $CdCl_2$ for 0, 1, 3, 6, 12, 24 h (B). mRNA expression was qualified for *BiP* (C) , *ATF4* (D)and *CHOP* (E) by qPCR after cells were exposed to indicated concentrations (0, 5, 10, and 20 μM) of $CdCl_2$ for 24 h. The translational level of CHOP was also detected by western blotting (F). (G) ARPE-19 cells were pretreated with or without NAC (2 mM) for 2 h and then treated with 20 μM $CdCl_2$ for 24 h. Then *BiP* was analyzed by qPCR. Each value is presented as mean ± SEM (n=3). ***$P < 0.001$; Con., Control. (H) ARPE-19 cells were exposed to 20 μM $CdCl_2$ for 24 h in the absence or presence of 4 mM Tempol, and then BiP and CHOP were detected by western blotting.

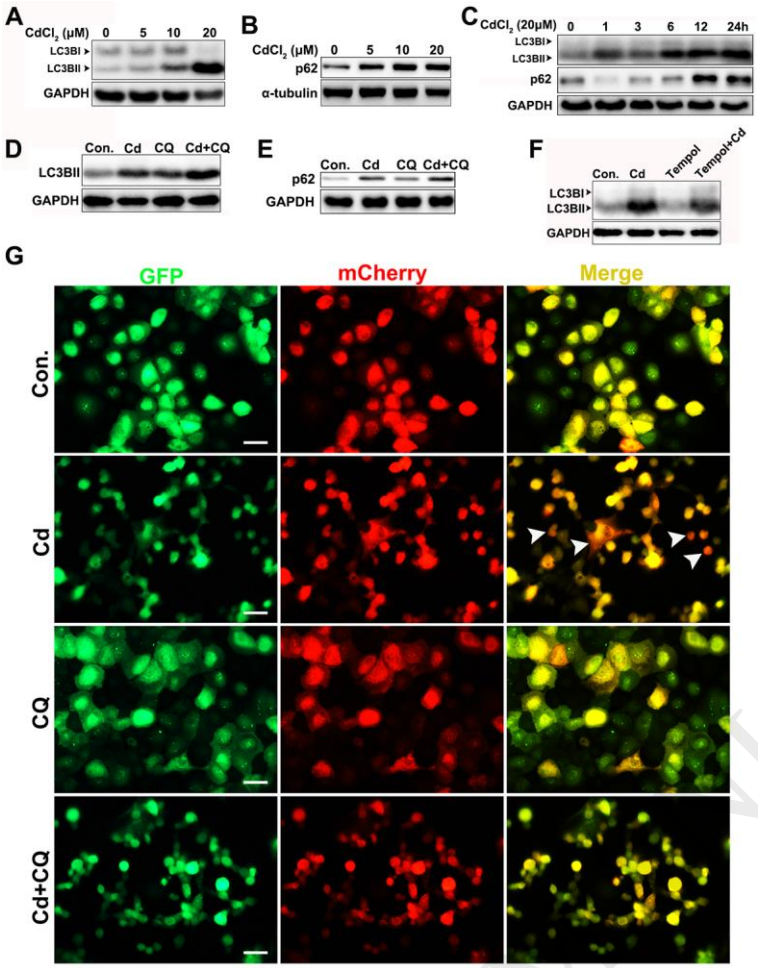

Fig. 3. Cd induces autophagy in RPE cells.

(A and B) After ARPE-19 cells were incubated with $CdCl_2$ (0-20 μM) for 24 h, immunoblotting for LC3BII and p62 were used to observe autophagy. (C) LC3BII and p62 expression were determined by western blotting after ARPE-19 cells were treated with 20 μM $CdCl_2$ for 0, 1, 3, 6, 12, 24 h. (D and E) ARPE-19 cells were pre-incubated 2 h with or without CQ (20 μM) and exposed to 20 μM $CdCl_2$ for 24 h. Then LC3BII and p62 were detected by immunoblotting. (F) Cells were incubated with 20 μM $CdCl_2$ for 24 h in the absence or presence of 4 mM Tempol, and immunoblotted for indicated proteins. (G) ARPE-19 cells were infected with recombinant adeno-associated virus vectors packing mCherry-EGFP-LC3B. After 24 h post-infection, cells

were then pre-incubated 2 h with or without CQ (20 μM) and exposed to 20 μM $CdCl_2$ for 24 h and analyzed by fluorescence microscopy.

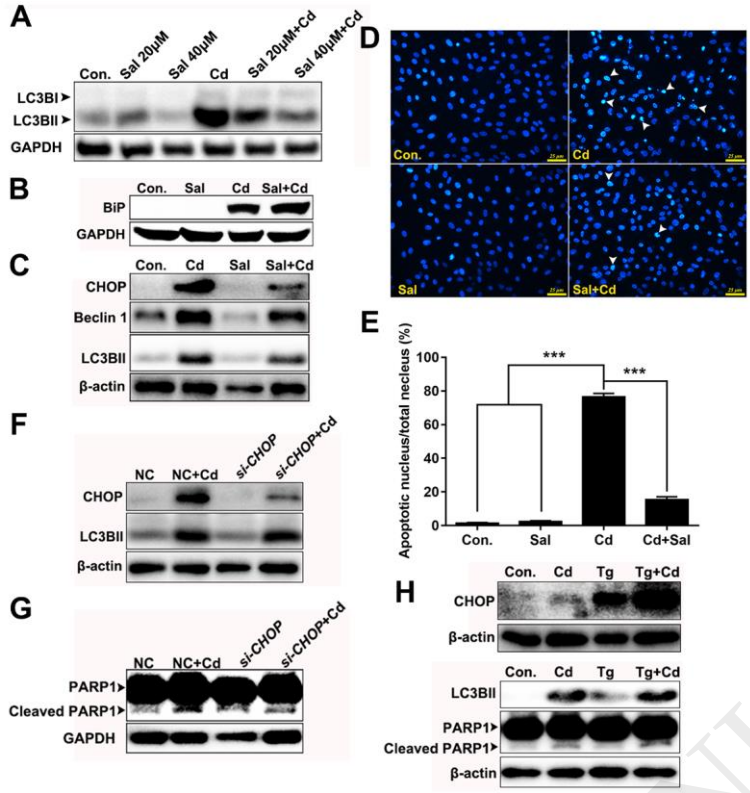

Fig. 4. ER stress contributed to Cd-induced autophagy and cytotoxicity in RPE cells.

(A–C) LC3BII, Beclin 1, BiP, and CHOP were determined by western blot after ARPE-19 cells were pretreated with or without salubrinal for 2 h and then incubated with 20 μM Cd for 24 h. (D) DAPI staining was used to detect the pyknotic nuclei in ARPE-19 cells following $CdCl_2$ (20 μM) treatment; white arrowheads indicate the nuclei apoptotic-like morphological changes. Scale bar, 50 μm; Con., Control. (E) Apoptotic nuclei/total nuclei was calculated and expressed as apoptosis rate in each group, each value is presented as mean ± SEM of 3 or 5 field of microscope. ***P < 0.001; Con., Control. (F and G) ARPE-19 cells were transfected with siRNA targeting CHOP (100 nM) for 24 h, and the protein level of CHOP, LC3B, and PARP1 were evaluated after Cd-exposure by western blot. NC, Negative control. (H) ARPE-19 cells were exposed to 20 μM $CdCl_2$ for 24 h in the absence or presence of Tg (1 μM), then total cell lysates were analyzed by western blotting using indicated antibodies.

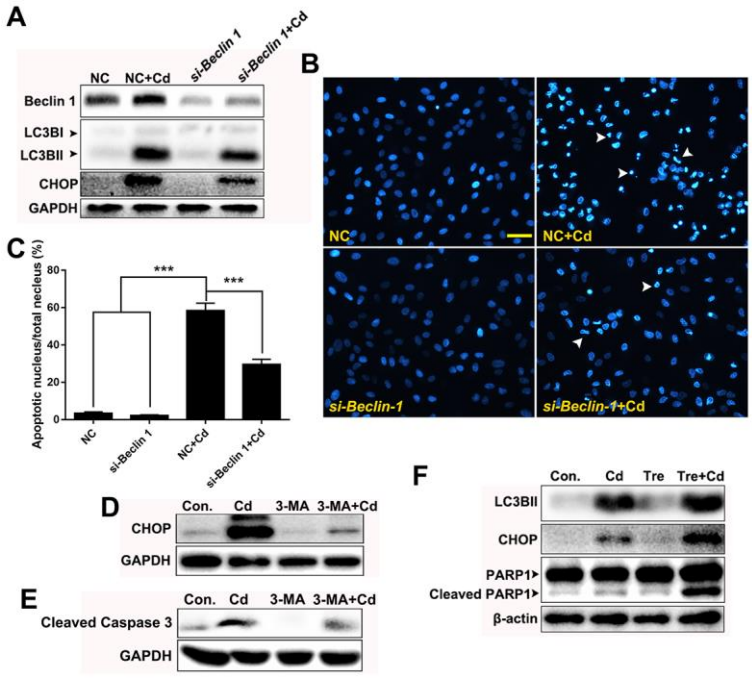

Fig. 5. Autophagy is involved in Cd-caused RPE cell death.

(A) ARPE-19 cells were transfected with siRNA targeting Beclin 1 (100 nM) for 24 h, and the protein level of Beclin 1, LC3B, and CHOP were evaluated after Cd-exposure by western blot. NC, Negative control. (B) DAPI staining was used to detect the pyknotic nuclei in ARPE-19 cells following $CdCl_2$ (20 μM) treatment; white arrowheads indicate the nuclei apoptotic-like morphological changes. Scale bar, 50 μm; NC, Negative control. (C) Apoptotic nuclei/total nuclei was calculated and expressed as apoptosis rate in each group, each value is presented as mean ± SEM of 3 or 4 field of microscope. ***$P < 0.001$; NC, Negative control. (D and E) CHOP and cleaved-caspase 3 was determined by western blot after ARPE-19 cells were exposed to 20 μM $CdCl_2$ for 24 h in the presence or absence of 5 mM 3-MA. (F) ARPE-19 cells were subjected to $CdCl_2$ in the presence or absence of 50 mM Tre for 24 h, and then the protein levels of LC3B, CHOP, and PARP1 were evaluated by western blot